Arabian Journal of Chemistry (2016) 9, 872–881

King Saud University

Arabian Journal of Chemistry

www.ksu.edu.sa
www.sciencedirect.com

ORIGINAL ARTICLE

Structural and physicochemical characterization and purity assessment of myrsinoic acids A and B, active compounds isolated from *Rapanea ferruginea* barks

Tailyn Zermiani [a], Ângela Malheiros [a], Ruth Meri Lucinda da Silva [a], Hellen Karine Stulzer [b], Tania Mari Bellé Bresolin [a,*]

[a] *Programa de Pós Graduação em Ciências Farmacêuticas e Núcleo de Investigações Químico-Farmacêuticas (NIQFAR)-Curso de Farmácia CCS/UNIVALI, Itajaí (SC), Brazil*
[b] *Laboratório de Controle de Qualidade, Departamento de Ciências Farmacêuticas, Universidade Federal de Santa Catarina, Brazil*

Received 29 April 2015; accepted 26 June 2015
Available online 10 July 2015

KEYWORDS

Myrsinoic acid A;
Myrsinoic acid B;
Structural and physicochemical characterization;
Stability indicating methods;
LC–UV method;
Purity

Abstract The present study provided a chemical, physical and physicochemical characterization of myrsinoic acids A (MAA) and B (MAB) isolated from stem bark of *Rapanea ferruginea* Mez (Myrsinaceae). In previous pre-clinical studies these compounds have shown important anti-inflammatory, anticholinesterasic and antimicrobial activities. A gradient stability-indicating LC–UV method was developed, and a forced degradation study was carried out. Purity, log *P*, solubility, and pK_a were determined. Thermal analysis (DSC/TG) was conducted for both compounds. MAB was characterized by X ray powder diffraction (XRPD) and scanning electron microscopy (SEM). When submitted to stress conditions, both markers showed degradation, with MAA presenting higher lability. The purity of MAA (oil) was 76.20%, while that of MAB (powder) was 98.90%. MAA and MAB exhibited log *P* values of 3.30 and 3.22, respectively. MAA was very slightly soluble in methanol and acetonitrile, while MAB was slightly soluble in both solvents. Both were practically insoluble in water. MAA and MAB showed pK_a of 4.5 and 4.8, respectively. In the SEM analysis, MAB showed a semi-crystalline morphology and high purity when analyzed by XRPD and DSC. This data will contribute to the development, quality control and standardization of pharmaceuticals using MAA and MAB.

* Corresponding author. Tel.: +55 (47)3249 7930.
E-mail address: tbresolin@univali.br (T.M.B. Bresolin).
Peer review under responsibility of King Saud University.

Production and hosting by Elsevier

1. Introduction

Prenylation consists of the addition of an isoprenoid side chain to another molecule (Alhassan et al., 2014). A wide range of pharmacological activities have been reported for prenylated

http://dx.doi.org/10.1016/j.arabjc.2015.06.032
1878-5352

benzoic acids' derivatives of secondary metabolites (Chen et al., 2000; Flores et al., 2009; Malami, 2012; Seeram et al., 1996). Phytochemical studies of the *Rapanea* genus have led to the isolation of diprenylated benzoic acids (Blunt et al., 1998) named myrsinoic acids A (3-geranyl-4-hidroxy-5-(3′methyl-2′-butenyl)-benzoic acid), B (5-carboxy-2,3-dihydro-2-(1,5-dimethyl-1 hydroxy-4-hexenyl)-7-(3-methyl-2-butenyl)benzofuran), C ((2S),(3S)-6-carboxy-2,3-dihydro-3-hidroxy-2-methyl-2-(4′-methylpenta-3′-enyl)-8-(3″-methyl-2″-butenyl)-cromon), E (3,5-digeranyl-4-hydroxy)-benzoic acid) and F (5-carboxy-2,3-dihydro-2-(1′,5′-dimethyl-1′E,4′-hexadienyl)-7-(3″-methyl 2″-butenyl)-benzofuran), which have shown important anti-inflammatory activities (Dong et al., 1999; Hirota et al., 2002; Ito et al., 2008; Makabe et al., 2003). The structural characterization by these authors consisted of NMR, IR and EIMS techniques.

The presence of myrsinoic acids A, B and C was previously identified in the extract of stem bark of *Rapanea ferruginea* Mez (Myrsinaceae) (syn. *Myrsine coriacea*) (Baccarin et al., 2011). These compounds showed anticholinesterasic activity (Gazoni, 2009) and presented significant antibacterial activity against *Staphylococcus aureus* and *Bacillus subtilis*. MAA and MAB also presented moderate toxic potential in the brine shrimp test and were not mutagenic in *Saccharomyces cerevisiae* (Bella-Cruz et al., 2013).

Myrsinoic acid A (MAA) Fig. 1A was an inhibitor of mammalian DNA polymerases (Mizushina et al., 2000). MAA showed facilitating action on the stages of memory (acquisition, consolidation and evocation) in normal mice, and also in mice with streptozotocin-induced Alzheimer's disease (Costa et al., 2003).

Myrsinoic acid B (MAB) Fig. 1B exhibited methioninase inhibitor activity from periodontal bacteria such as *Fusobacterium nucleantum*, *Porphyromonas gingivalis* and *Treponema denticola* (Ito et al., 2008). In addition, this compound showed a significant antinociceptive effect through mechanisms that involve interaction with L-arginine–nitric oxide, the serotonergic and cholinergic systems, and the α-adrenoceptors (Hess et al., 2010). MAB administered preventively or therapeutically, systemically or by the spinal route, reduced mechanical and thermal hypersensitivity in mice submitted to models of inflammatory and neuropathic pain, shows an excellent potential to treat persistent pain in humans, without any significant side effects (Antonialli et al., 2012). MAB exhibited pronounced leishmanicidal activity against *Leishmania amazonensis* and *Leishmania brasiliensis*, suggesting its importance as a possible source of antiparasitic agents (Cechinel-Filho et al., 2013).

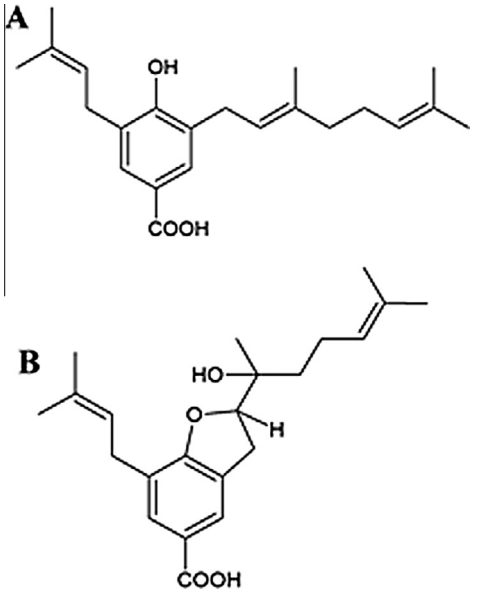

Figure 1 Structures of the myrsinoic acids A (A) and B (B).

Considering the absence of physicochemical data and the potential application of MAA and MAB as phytodrugs, or possible drug leads, suitable for future optimization by medicinal and synthetic chemists, the aim of this study was to provide a chemical, physical and physicochemical characterization of these compounds to assist in the quality control of its related pharmaceutical products.

2. Material and methods

2.1. Chemicals and reagents

Analytical grade hexane and ethyl acetate were purchased from Vetec (Rio de Janeiro, Brazil). Deuterated chloroform ($CDCl_3$) was purchased from Merck (White House Station, NJ, USA).

For HPLC analysis, all solvents used were HPLC grade (Tedia, Fairfield, Ohio, USA). The water was purified using a Milli-Q system (Millipore, Massachusetts, USA). All solutions were filtered through 0.45 μm membrane (Millipore, Massachusetts, USA).

2.2. Isolation and purification of myrsinoic acids A and B

Isolation procedures were performed according to Hess et al. (2010) and Bella-Cruz et al. (2013) as briefly described below: a mixture of hydroethanolic extracts of stem bark, branches and leaves of *R. ferruginea* (43 g) was subjected to silica gel column chromatography with hexane/ethyl acetate to obtain myrsinoic acids A and B in their pure forms. The fractions eluted with 20% and 40% of ethyl-acetate in hexane gave MAA (2.3 g), and MAB (4.2 g), respectively. After solvent evaporation, MAA presented as a yellow oil, and MAB as a crystalline white powder.

2.3. Structural characterization

2.3.1. Nuclear magnetic resonance ^{1}H and ^{13}C

NMR spectra were measured on a Bruker AC-300F® 300 MHz. Hydrogen nuclear magnetic resonance (^{1}H NMR) and Carbon-13 nuclear magnetic resonance (^{13}C NMR) spectra were recorded using $CDCl_3$ as solvent. Chemical shifts were referenced to the residual solvent peak, or to tetramethylsilane (TMS) as an external reference. The data were reported in terms of chemical shift (δ, in ppm), multiplicity, coupling constant (J, in Hz), and integrated intensity. The multiplicity of a particular signal was indicated as s (singlet), d (doublet), t (triplet), or m (multiplet).

2.3.2. Fourier transform infrared spectroscopy (FTIR)

FTIR spectra were recorded on a FT-IR Shimadzu® IR Prestige-21. A fourier transform infrared spectroscopy

equipped with an attenuated total reflectance (ATR) accessory was used to obtain infrared spectra of MAA. FTIR analysis of MAB was carried out using diffuse reflectance spectroscopy DRS-FTIR with KBr. Each spectrum was obtained from 3600 to 700 cm^{-1}.

2.3.3. Raman spectroscopy

The Raman experiment was carried out in a PeakSeeker 785 (RAM-PRO-785). The Raman system was operated with a diode laser of 785 nm and 300 mW at the source. The collected Raman radiation was dispersed with a grating and focused on a Peltier-cooled charge-coupled device allowing a spectral resolution of 6 cm^{-1} to be obtained. The laser was focused on the sample by the 4× objective lens of a microscope, giving a spot of approximately 2 μm diameter. All spectra were recorded in the spectral window of 200–1800 cm^{-1} with the same acquisition time (30 s). The MAB sample was analyzed on a glass slide at room temperature.

2.3.4. Ultraviolet spectroscopy

UV spectra were measured in samples at a concentration of 50 μg mL^{-1} using methanol as solvent. Specific absorption ($E^{1\%}_{1cm}$) was calculated at 260 nm for MAA, and 270 nm for MAB.

2.3.5. Mass spectrometry with direct sample inlet (DI-MS)

MS spectra were measured on a Shimadzu DI-2010 direct sample inlet accessory that was attached to a GC2010 GC/MS (Shimadzu, Kyoto, Japan). The mass spectrometer was operated in electron ionization positive mode. The sample was directly introduced into the ion source, for which the temperature was set to 250 °C.

2.4. HPLC analysis

Chromatographic analysis was carried out on a HPLC Shimadzu® LC 20-AT system, consisting of a quaternary pump and a Shimadzu SPD-M20A photodiode array detector, SIL-20A HT auto-sampler, with a Shimadzu CTO-10AS VT column oven equilibrated at 35 °C, and software LC Solution was used. The chromatographic column used was Phenomenex Kinetex® C_{18} column (150 × 4.6 mm) with core-shell particles of 2.6 μm. The separation was achieved on a gradient method. The method was chosen according to the best separation of myrsinoic acids A and B at a concentration of 50 μg mL^{-1} in methanol solution. The best mobile phase was methanol–acetonitrile–water (acidified to pH 2.5 with phosphoric acid) at a flow rate of 0.9 mL min^{-1}. The gradient elution was programmed as follows: initial isocratic condition during 2 min (25:5:70), 2–5 min (25:30:45), 5–10 min (25:60:15), 10–12 min (20:70:10), 12–15 min (15:75:10) and 15–20 min (15:84:1) then returns to the initial condition until 30 min of analysis. The analysis was monitored at 260 nm for MAA and at 270 nm for MAB. The purity of MAA and MAB was calculated through the presence of other peaks in the chromatograms of the compounds, expressed in relative area.

The specificity of the method was established according to the ICH guidelines (2005) using the PDA detector for the peak purity evaluation, and the samples were analyzed under forced degradation conditions (acidic, alkaline, oxidative and photodegradation), as described below.

2.5. Stability data

In order to develop a gradient stability-indicating LC–UV method, a forced degradation study of MAA and MAB was carried out. Both compounds were initially dissolved in methanol (50% of the volume) and the volume was made up with the degraded solutions as follows: hydrolytic stress studies were performed (at 25 °C) in acid (1 M HCl, 24 h), basic (1 M NaOH, 24 h) and oxidative (30% H_2O_2, 6 h) conditions, at final concentration of 100 μg mL^{-1} solutions of MAA and MAB. The MAA oil and MAB powder were submitted under conditions of visible light (2.4 mi lux h^{-1}) and UVA (400 W h m^{-2}) irradiation. After exposure, sample solutions of 100 μg mL^{-1} in methanol were analyzed by the HPLC method. The stressed samples were assayed by comparison with non-degraded reference standards.

To confirm the temporal stability of MAA and MAB in methanol and acetonitrile, 2.5 mg of each sample was weighted and dissolved in 25 mL of each solvent. The solutions were stored in the following three conditions: light shielding at room temperature, light shielding at 15 °C and light shielding at 2 °C. The sampling periods were 0, 4, 8, 24, 48 h and 14 days. Each sample was evaluated by HPLC. Statistical analysis was carried out by one-way ANOVA using experimental design tools of Statistica® 6.0 software followed by Tukey test. The level of significance used was $p < 0.05$.

2.6. Physicochemical characterization

2.6.1. Log P

The octanol/water partition coefficient (log *P*) was measured according to OECD guideline n. 117 (1989), which uses the HPLC technique. The reference substances used were benzyl alcohol, phenol, benzoic acid, benzene, toluene and naphthalene. The injections (20 μL) were carried out on a Phenomenex (Torrance, California, USA) C18 3 μm Fusion RP 100 Å (150 mm × 4.6 mm), the mobile phase consisted of 80:20 (v/v) methanol–water (pH 3.00, phosphoric acid) and the elution occurred in isocratic conditions, at a flow rate of 1.0 mL min^{-1}, and detection at 210 nm. Capacity factors (*k*) of each substance were obtained by the following expression:

$$k = \frac{t_R - t_0}{t_0}$$

where t_R is the retention time of the test substance, and t_0 is the dead-time. The *k* value and their respective log *P* were correlated on analytical curve (log *k* *versus* log *P* of the reference substances) and analyzed by linear regression. To determine the myrsinoic acids A and B log *P*, solutions with concentration of 50.0 μg mL^{-1} were injected in the same chromatographic conditions, and the *k* value of each compound was determined and then input into the straight line equation.

2.6.2. Solubility

The solubility of myrsinoic acids A and B was designed to comply with pharmacopoeic specifications (The United States Pharmacopeia, 2012). This parameter was tested for methanol, acetonitrile and water. Increasing amounts of each standard were added to a fixed volume of solvents to obtain saturated solutions. The supernatant was filtered through a 0.45 μm filter. The drug concentration was determined by HPLC (Section 2.4).

2.6.3. pK_a prediction

Conformational analysis was carried using the Spartan software (Wavefunction Inc., Irvine, California, USA). Density Functional Theory (DFT) was performed on Gaussian 09 software. The pK_a prediction was performed using Maestro, version 9.4 (Schrodinger New York, NY, 2013) software.

2.6.4. Thermogravimetry (TG) and differential scanning calorimetry (DSC)

For the thermal analysis, a DSC/TG Netzsch STA 449 F3 Jupiter® was used. The TG and DSC studies were carried out with a simultaneous DSC/TG apparatus thermal analyzer, at 1 °C min^{-1}, from 20 °C to 450 °C. Dry nitrogen at a flow rate of 50 mL min^{-1} was used as the purge gas. Alumina crucibles were used as the sample holder (5 mg).

2.6.5. X-ray powder diffraction (XRPD)

X-ray diffraction patterns of MAB were obtained using a θ–θ-ray diffractometer (Xpert Pro Multi-Purpose Diffractometer, PanAnalytical) equipped with Kα copper radiation (λ = 1.5418 Å), operating with 40 mA current and 45 kV voltage, sample spinner and a Real Time Multiple Strip (RTMS) detector. The measurements were taken at room temperature, scanning 2θ from 4° to 35°, with a 0.016 step size and 25.0 s step time.

2.6.6. Scanning electron microscopy

Due to the fact that MAA is an oil, SEM analyses were possible only for MAB powder. The sample surface was coated with a layer of gold with a thickness of 8–10 nm by sputtering using a Baltec (Liechtenstein, Switzerland) SCD 005 equipment, and then analyzed in a Philips (Hillsboro, U.S.A.) XL 30 electron microscope with a voltage of 10 kV. Photomicrographs were taken with 105, 500 and 1000-fold magnification.

3. Results and discussion

In addition to the chemical characterization of MAA and MAB we carried out physicochemical and stability studies. The latter studies are more commonly applied to synthetic or nanocomposites (Hattab and Benharrats, 2015); however, the importance of this characterization of natural compounds relates to their potential as phytodrugs or even as leading molecules to optimization in pharmaceutical chemistry, aiming the improvement of its pharmacodynamic/pharmacokinetic aspects.

3.1. Structural characterization

In order to confirm the chemical structure of MAA and MAB, it was carried out the spectroscopic and spectrometric analysis of NMR (^{1}H and ^{13}C), FTIR and UV. In addition, it was determined, for the first time, the fragmentation patterns by mass spectrometry and the Raman spectroscopy.

3.1.1. Nuclear magnetic resonance ^1H and ^{13}C

Spectral Data for AMA: ^{1}H NMR ($CDCl_3$, 300 MHz) δ: 1.60 (3H, s, H-10′), 1.69 (3H, s, H-8′), 1.77 (9H, s, H-4″, 5″, 9′), 2.11 (2H, m, H-5′), 3.38 (2H, t, J = 6.0 Hz), 3.39 (2H, t, J = 6.0 Hz), 5.08 (1H, m, H-6′), 5.32 (2H, t, J = 7.0 Hz, 2H′, 2″), 7.77 (2H, s, H-2, H-6). ^{13}C NMR ($CDCl_3$, 75,5 MHz) δ: 16.2 (C-9′), 17.9 (C-10′, 4″), 25.7 (C-8′), 25.8 (C-5″), 26.3 (C-5′), 29.3 (C-1″), 29.7 (C-1′), 39.7 (C-4′), 121.0 (C-1), 121.2 (C-2′), 121.4 (C-2″), 123.8 (C-6′), 127.0 (C-3, C-5), 130.5 (C-2, C-6), 131.8 (C-7′), 134.0 (C-3″), 139.1 (C-3′), 158.0 (C-4), 172.0 COOH.

Spectral Data for AMB: ^{1}H NMR ($CDCl_3$, 300 MHz) δ: 1.30 (3H, s, H-7′), 1.55 (2H, m, H-2′), 1.63 (3H, s, H-8′), 1.69 (3H, s, H-6′), 1.72 (3H, s, H-5″), 1.73 (3H, s, H-4″), 2.17 (2H, m, H-3′), 3.17 (2H, dd, J = 16.0, 9.2 Hz, H-3), 3.29 (2H, m, H-1″), 4.74 (1H, t, J = 9.2 Hz, H-2), 5.12 (1H, t, J = 7.2 Hz, H-4′), 5.28 (1H, t, J = 7.2 Hz, H2″), 7.75 (2H, s, H-4, H-6). ^{13}C NMR ($CDCl_3$, 75.5 MHz) δ: 17.7 (C-8′), 17.9 (C-5″), 22.0 (C-3′), 22.6 (C-7′), 25.6 (C-4″), 25.7 (C-6′), 28.3 (C-1″), 29.9 (C-3), 37.1 (C-2′), 73.8 (C-1′), 89.6 (C-2), 121.4 (C-2″), 121.8 (C-5), 123.1 (C-3a), 124.0 (C-4′), 125.0 (C-6), 127.2 (C-7), 131.4 (C-4), 132.2 (C-5′), 133.2 (C-3″), 162.4 (C-7a), 171.7 (C8).

The NMR ^{1}H and ^{13}C spectral data obtained for myrsinoic acids A and B were consistent with the literature (Bella-Cruz et al., 2013; Hess et al., 2010; Hirota et al., 2002; Makabe et al., 2003).

Since the structure of MAB presents two chiral centers, 2D Nuclear Overhauser Effect Spectroscopy (NOESY) and proton nuclear magnetic resonance spectroscopy (NMR) were applied, to determine the relative configurations of the diastereomers (see supplementary material).

3.1.2. Fourier transform infrared spectroscopy (FTIR)

The MAA ATR-FTIR spectrum, presented in Fig. 2A, showed absorption peaks at 2918 cm^{-1}, corresponding to CH_{sp3} stretch. A broad overlapping OH band in the range of 3400–2600 cm^{-1} was observed, which together with the peak at 1678 cm^{-1} (C═O), characterizes the carboxylic acid. At 1600 cm^{-1} and 1201 cm^{-1}, the peaks observed correspond to the C═C and C—O stretch. The DRS-FTIR spectrum for MAB, shown in Fig. 2B, displayed a stretch peak at 3367 cm^{-1} with O—H corresponding to alcohol. A prominent absorption band between 3000 and 2600 cm^{-1} and intense peak at 1701 cm^{-1} correspond to carboxylic acid. The peak at 1605 cm^{-1} corresponds to the C═C stretch, confirmed by the intense bending peak at 960 cm^{-1}. The 1282 and 1180 cm^{-1} bands correspond to the C—O stretch, concerning aryl-alkyl-ether in the molecule.

3.1.3. Raman spectroscopy

Raman spectroscopy is an analytical technique that is widely applied to the chemical and physicochemical characterization of solid compounds as it is a non-destructive method and needs only minimal sample preparation. Furthermore, in contrast to IR spectroscopy, it is not disturbed by the presence of water. Raman spectra are a highly specific method, serving as the fingerprints of the molecules (Láng et al., 2013). Raman spectroscopy was performed complementary to DRIFT, with the purpose of elucidating and confirming the compound structure. The MAB Raman spectrum is presented in Fig. 3. It showed the main characteristic bands at 1700–1500 cm^{-1}, relating to the aromatic ring and COOH vibrations, respectively, in 1400 cm^{-1} the vibration relative to CH_3CH_2, and the double bond signal is demonstrated at 1300 cm^{-1}, which is in agreement with the previous data (Vandenabeele et al., 2000).

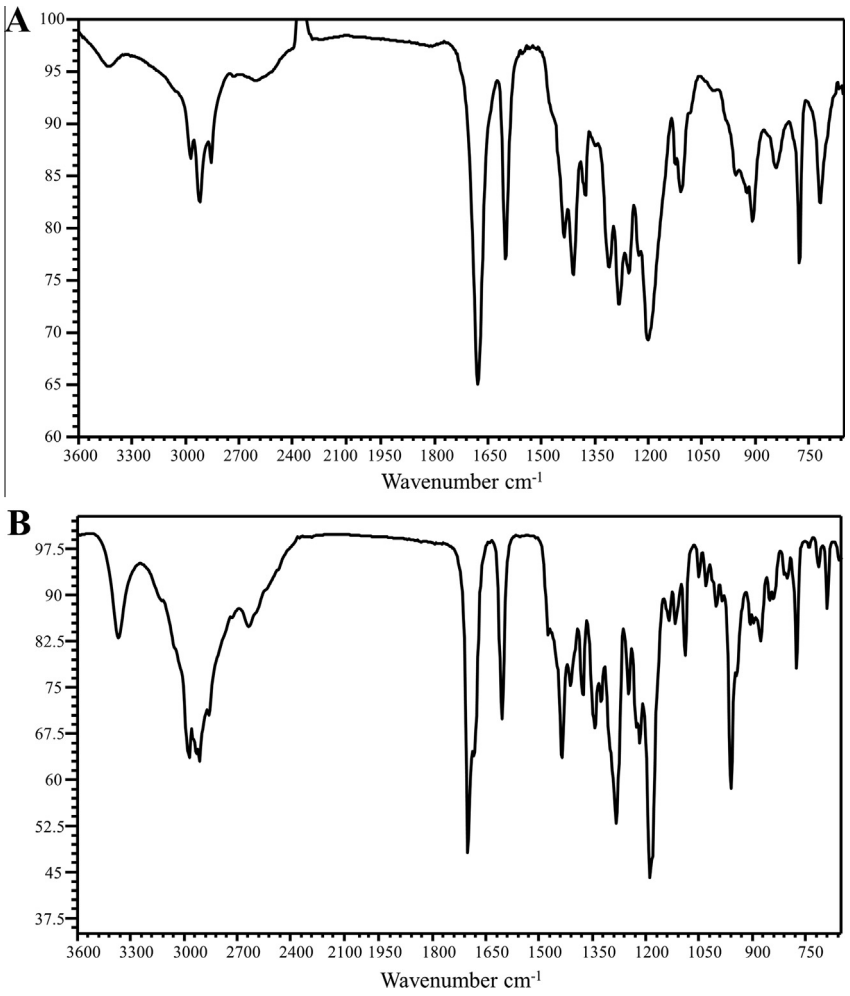

Figure 2 FTIR spectra of myrsinoic acid A (A) and myrsinoic acid B (B).

3.1.4. Ultraviolet spectroscopy

The MAA UV spectrum (Fig. 4) presented two maximum absorption peaks, at approximately 205 and 258 nm. MAB showed maximum absorption at 218 and 269 nm (Fig. 4). Specific absorption ($E^{1\%}_{1cm}$) was 287.2 and 229.0 for MAA and MAB, respectively.

3.1.5. Mass spectrometry with direct sample inlet (DI-MS)

The insertion of MAA into the mass spectrometer resulted in a spectrum (Fig. 5A) with a molecular ion peak at *m*/*z* 342 and a base peak at *m*/*z* 123, which was generated by cleavage between C1′ and C2′ bond (C_9H_5). The MAB mass spectrum (Fig. 5B) showed the molecular ion peak at *m*/*z* 358 and the base peak at *m*/*z* 69 corresponding to the fragment (C_5H_9), generated by the cleavage of the C1″ and C7 bond. For this compound, an intense peak was observed at *m*/*z* 109, which is suggestive of the C1′ and C2 cleavage bond, with loss of water.

3.2. HPLC analysis

The HPLC method was developed considering the parameters of resolution factor (*R*) between peaks, runtime and the capacity of being stability-indicative. The use of an acid mobile phase was required. MAA and MAB had retention times (R_T) of 16.03 ± 0.01 and 15.47 ± 0.01 min, respectively (Fig. 4). Separation was considered satisfactory (R = 4.3). The calculated purity of MAA was 76.20% and MAB of 98.90%. It was not observed supplementary peaks in another wavelength (200–400 nm), for both compounds. The HPLC method showed good specificity, as the peak purity through

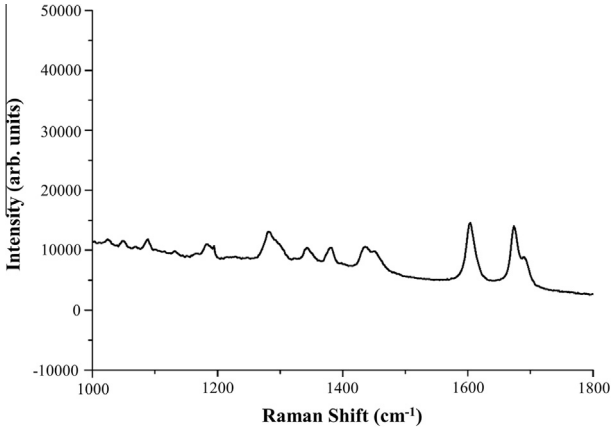

Figure 3 Raman spectrum of MAB.

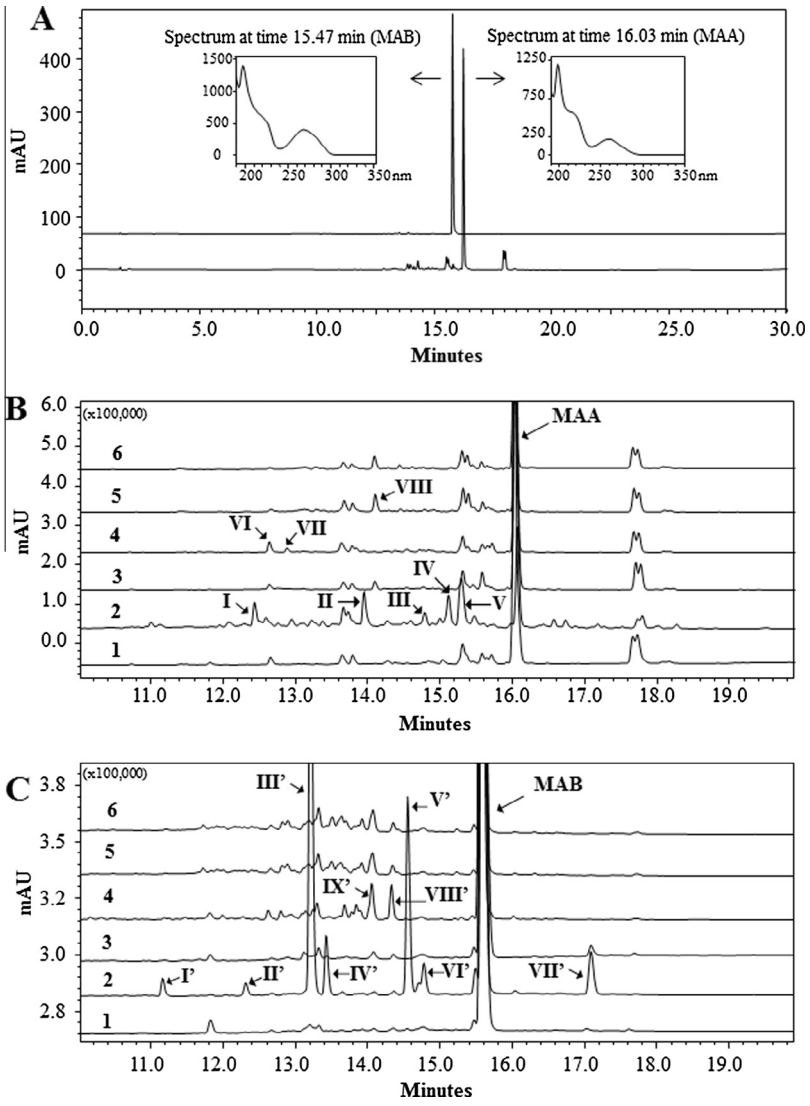

Figure 4 (A) Chromatographic profiles of MAA at 260 nm (R_T of 16.03 min), and of MAB at 270 nm (R_T of 15.47 min) and its respective UV spectra; Chromatographic profiles of MAA at 260 nm (B) and MAB at 270 nm (C) after degradation studies: (1) non-degraded samples at 100 μg mL^{-1}; (2) samples after stress with 1 M HCl 24 h; (3) samples after stress with 1 M NaOH 24 h; (4) samples after stress with 30% H_2O_2 6 h; (5) samples after stress with visible light (2.4 mi lux h^{-1}); (6) and samples after stress with UVA (400 W h m^{-2}).

PDA was >99.99% for both compounds, and there was not apparent co-elution of degradation products with MAA and MAB peaks after the stress tests described below.

3.3. Stability data

After dissolved in the degraded solutions, both compounds remained visually soluble. Significant degradation was observed after acid hydrolysis (1 M HCl, 24 h) of MAA (72.22%) and MAB (43.44%). Chromatographic profile of degraded MAA showed the presence of at least six different impurities with R_T between 12.4 and 15.3 min, as observed in Fig. 4A-2. The MAB chromatogram after acid hydrolysis presented seven impurity peaks between 11.2 and 17.1 min (Fig. 4B-2).

Degradation was not observed when MAA and MAB were exposed to alkaline hydrolysis condition (Fig. 4A-3 and B-3, respectively), probably due to the formation of a stable salt.

MAA submitted to oxidative hydrolysis (30% H_2O_2, 6 h), showed significant degradation (36.60%), and supplementary peaks were observed at about 12.63 and 12.88 min (Fig. 4A-4). MAB exposed to the same conditions exhibited degradation of 6.80%, and supplementary peaks were detected at 14.06 and 14.33 min (Fig. 4B-4).

After visible light exposure (2.4 mi lux h^{-1}) of the MAA sample, the yellowness of the oil decreased. Its chromatographic analysis showed a significant degradation of 40.74% and a different peak with R_T about 14.0 min (Fig. 4A-5). When MAB was submitted at this stress condition, a color change was observed in the white powder, which turned yellow. The HPLC profile, presented in Fig. 4B-5, showed a MAB degradation of 29.93% and elution of the degradation products at between R_T 12.8 and 14.6 min. When MAA was exposed to UVA irradiation (400 W h m^{-2}), the oil presented a dark yellow coloration and degradation of 45.01% was

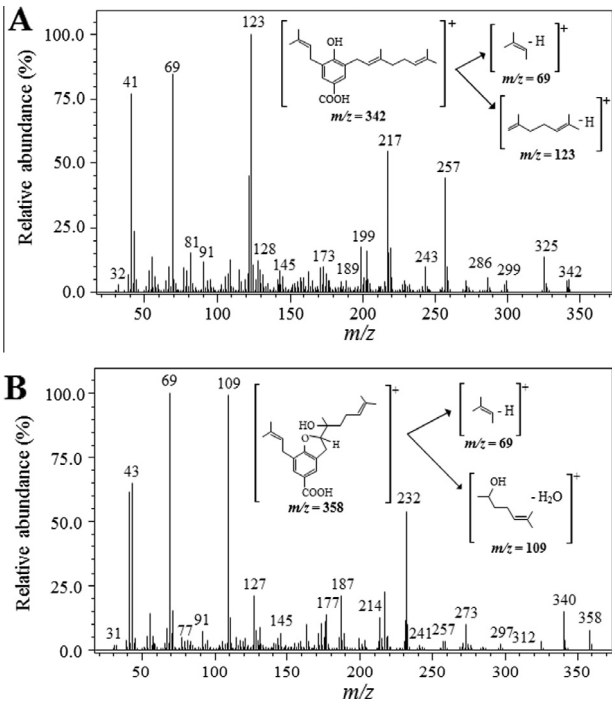

Figure 5 DI-MS (EI mode) mass spectrum of MAA (A) and MAB (B) and suggested major fragmentation mechanisms.

observed. As observed in Fig. 4A-6, the same impurities were observed, which appeared after visible light exposure, at R_T of 14.08 min. MAB presented color change to dark yellow after UV exposure. This compound also had significant degradation (21.97%), and the same degradation products were observed at between R_T 12.8 and 14.6 min (Fig. 4B-6), for the MAB after visible light exposure.

The temporal stability test indicates that the MAA and MAB methanol solutions were stable when stored at light shielding at room temperature until 14 days. MAB acetonitrile solutions showed stability at the room temperature, after 14 days. However significant degradation of MAA acetonitrile solution was observed after 14 days, and no change in the chromatographic profile of MAA, probably due to the formation of nonchromophore degradation products.

Both MAA and MAB in methanol or acetonitrile solutions were stable until 14 days, when stored at light shielding at 2 °C or 15 °C. The statistical results showed no significant difference among samples. The RSD (%) for assay of MAA and MAB during solution stability was within $<2\%$.

3.4. Physicochemical characterization

Using HPLC, the partition coefficients ($\log P$) of each compound were determined by plotting the $\log P$ values against ($\log k$) of the known compounds (Fig. 6) (OECD, 1989), where t_0 was 3.31 min.

The following calibration curve was obtained: $\log P_{ow} = 2.1311 \cdot \log k + 2,244$ $(r^2 = 0.8773, n = 6)$. MAA and MAB exhibited $\log k$ values of $+0.52$ and $+0.48$, in that order, and the $\log P$ values were 3.30 and 3.22, respectively.

These data are extremely useful in the drugs biopharmaceutical classification. The literature reports that compounds with $\log P$ of between 2 and 3 show optimum skin permeability coefficient values (Hadgraft et al., 2000). Log P values found for MAA and MAB were similar to those of non-steroidal anti-inflammatory agents (NSAIDs) such as diclofenac, ibuprofen, indomethacin and naproxen, which showed significant skin permeability after topical application (Hadgraft et al., 2000; Singh and Roberts, 1994).

Lipophilicity is one of the most important descriptors to be identified for CNS penetration. Blood-brain barrier (BBB) penetration is considered optimal when the $\log P$ values are in the range of 1.5–2.7, with a mean value of 2.1 (Pajouhesh and Lenz, 2005). However, it is seen that CNS drugs differed considerably in their lipophilicity, not following this rule. For example, some antidepressants present a mean $\log P$ of 3.10 (Ghose et al., 1999), as well as some drugs used in the treatment of Alzheimer's disease, such as donepezil ($\log P$ value of 3.08–4.11) (Sozio et al., 2012) and Memantine, which has a $\log P$ value of 3.28 (Sonkusare et al., 2005). Thus, the $\log P$ of MAA can support the effects on memory observed in a previous study conducted by our research group (Costa et al., 2003). The absorption, excretion, and physiological barrier penetration may be related to the $\log P$ and pK_a values of drug, highlighting the importance of predicting both of these parameters in drugs.

TGAs of MAA revealed no mass loss from the sample over temperature range of 20–150 °C (Fig. 7A). Upon heating, MAA displayed a gradual loss of mass between 160 °C and 400 °C, maintained until 450 °C. The results evidence the low humidity of 1.42 ± 0.75% for this compound. The DSC thermogram for MAA showed an exothermic event at 272.1 ± 9.09 °C (Fig. 7A), characteristic of the process of thermal decomposition that occurs concomitant to heat release. As myrsinoic acid A is an oil, it was not possible observe its melting peak; thus, purity could not be ascertained using DSC.

The TGA plot of MAB shows that thermal degradation of the sample starts at 250 °C, with a progressive loss of mass until 350 °C, maintained up to 450 °C (Fig. 7B). The MAB humidity was 0.75 ± 0.01%. The DSC thermogram showed a sharp endothermic peak with maximum at 123.6 ± 0.1 °C, due to the compound melting (Fig. 7B). The exotherm event at 298.6 ± 10.3 °C corresponded to significant loss of mass and thermal degradation. The purity of MAB was determined as 100.74 ± 0.18 mol%, by the Van't Hoff equation.

The active pharmaceutical ingredient (API) can exist in different crystalline forms. Formulators should take advantage of

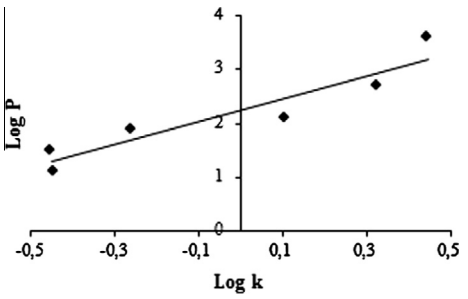

Figure 6 Correlation between $\log P$ and $\log k$ was determined by the isocratic method for reference compounds: benzyl alcohol, phenol, benzoic acid, benzene, toluene and naphthalene.

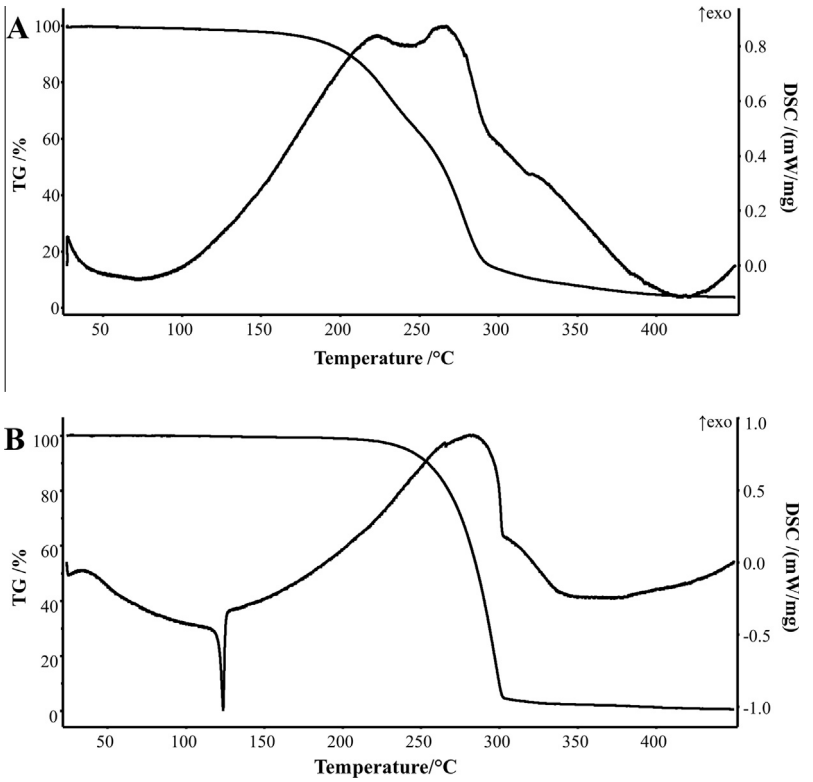

Figure 7 DSC and TG thermograms of MAA (A) and MAB (B).

this, where appropriate, when some unfavorable technological and biopharmaceutical properties of APIs need to be improved. The literature contains many examples of the suitability of using one crystalline form as opposed to another (Martino et al., 2007). In general, amorphous structure presents greater solubility than crystalline form, which is a desirable characteristic for a new pharmaceutical compound. As an example, low levels of amorphous character induced in griseofulvin by milling, increased its solubility of twofold or more (Elamin et al., 1994). The X-ray diffraction patterns related to myrsinoic acid B are shown in Fig. 8A. According to the diffractograms, it is possible to observe a semi-crystalline behavior for the sample, with an evident reflection at 5.2°, at low 2θ angles. These results, taken together with the DSC data, indicate that the phenolic compound MAB presents a semi-crystalline structure, what means that the sample has two phases, crystalline and amorphous.

The morphological analysis of drugs is an easy way to monitor and detect changes related to variations in crystal synthesis process or even in pharmaceutical processing (Maximiano et al., 2010). The photomicrograph of Fig. 8B shows the morphology of MAB crystallized by a solution of hexane–ethyl acetate (8:2) evaporated at room temperature with magnification of 1000×. It indicates a semi-crystalline compound, with the presence of some crystals with an orthorhombic appearance and particles without defined shape, which is

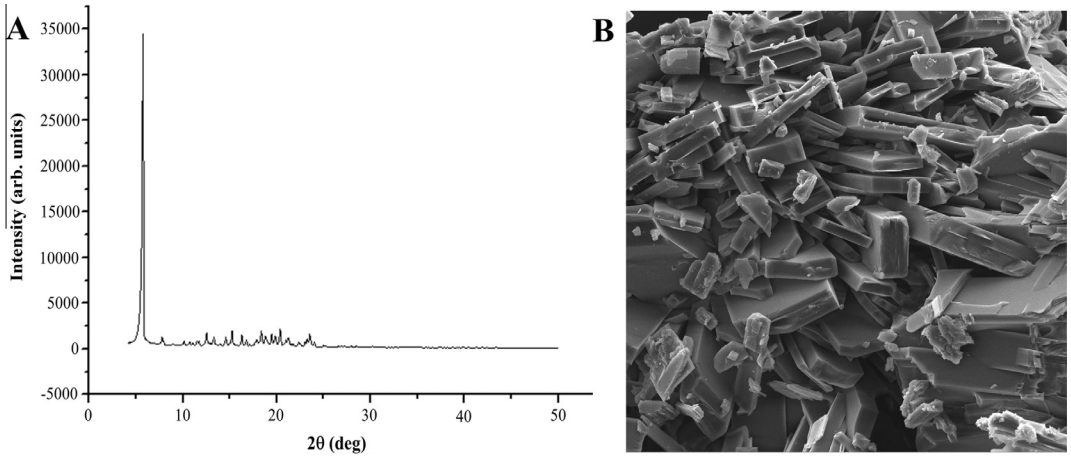

Figure 8 X-ray diffraction spectra (A) and SEM photomicrograph (enlargement of 1000×) (B) of MAB powder.

characteristic of an amorphous compound, and is in agreement with the previous results (DSC and XRPD).

Finally, the solubility analysis of markers revealed that MAA was very slightly soluble in methanol and acetonitrile, while MAB was slightly soluble in both solventes. Both markers were practically insoluble in water.

4. Conclusions

Knowledge of the chemical, physical and physicochemical properties of MAA and MAB characterized in the present study will enable the use of these compounds as analytical standards, and will contribute to the development and quality control of new phytodrugs. This information will also contribute to preformulation studies and the prediction of pharmacokinetic properties.

Acknowledgments

The authors thank the Laboratory (LDRX) of the Physics Department of the Federal University of Santa Catarina (UFSC) for carrying out the X-ray diffraction, and the Center for Electron Microscopy of the at the Federal University of Paraná (UFPR) for conducting the SEM analysis, to Tiago Bonomini for help with pKa determination and Theodoro Marcel Wagner for assistance with DI-MS analysis. The authors are also thankful to CAPES (Coordenação de Aperfeiçoamento de Pessoal de Nível Superior), Brazil, for providing financial support in the form of a master's degree scholarship to Zermian, T., CNPq (Conselho Nacional de Desenvolvimento Científico e Tecnológico), and FAPESC (Fundação de Amparo à Pesquisa e Inovação do Estado de Santa Catarina) (Edital PRONEM, 2708/2012).

Appendix A. Supplementary material

As presented in Fig. 9A, NOESY correlations were observed from H-2 to H-7′, H-2′ and H-3′. This demonstrates that the hydrogens H-2 and H-7′ are on the same side of the molecule. NOESY correlations from H-2′ to H-3′ and to H-4′, and from H-3′ to H-7′ were also observed. Based on a 2D NOESY experiment, two possible relative configurations were deduced, as shown in Fig. 9B. Supplementary data associated with this article can be found, in the online version, at http://dx.doi.org/10.1016/j.arabjc.2015.06.032.

References

Alhassan, A.M., Abdullahi, M.I., Uba, A., Umar, A., 2014. Prenylation of aromatic secondary metabolites: a new frontier for development of novel drugs. Trop. J. Pharm. Res. 13, 307–314.

Antonialli, C., Silva, G.F., Rocha, L.W., Monteiro, E.R., Souza, M.M., Malheiros, A., Yunes, R.A., Quintão, N.L.M., 2012. Antihyperalgesic effects of myrsinoic acid B in painlike behavior induced by inflammatory and neuropathic pain models in mice. Anesth. Analg. 115, 461–469.

Baccarin, T., Muceneeki, R.S., Bresolin, T.M.B., Yunes, A.R., Malheiros, A., Lucinda-Silva, R.M., 2011. Development and validation of an HPLC-PDA method for the determination of myrsinoic acid B in the extracts of *Rapanea ferruginea* Mez. Talanta 85, 1221–1224.

Bella-Cruz, A., Kazmierczak, K., Gazoni, V.F., Monteiro, E.R., Fronza, L.M., Martins, P., Yunes, R.A., Bürger, C., Tomio, T.A., Freitas, R.A., Malheiros, A., 2013. Bio-guided isolation of antimicrobial compounds from *Rapanea ferruginea* and its cytotoxic and genotoxic potential. J. Med. Plants Res. 7, 1323–1329.

Blunt, S.B., Chen, T., Wiemer, D.F., 1998. Prenylated Benzoic Acids from *Rapanea myricoides*. J. Nat. Prod. 61, 1400–1403.

Cechinel-Filho, V., Meyre-Silva, C., Niero, R., Mariano, L.N.B., Nascimento, F.G., Farias, I.V., Gazoni, V.F., Silva, B.S., Giménez, A., Gutierrez-Yapu, D., Salamanca, E., Malheiros, A., 2013. Evaluation of antileishmanial activity of selected brazilian plants and identification of the active principles. Evid. Based Complement. Altern. Med. 2013, 1–7.

Chen, B., Kawazoe, K., Takaishi, Y., Honda, G., Itoh, M., Takeda, Y., Kodzhimatov, O.K., Ashurmetov, O.J., 2000. Prenylated benzoic acid derivatives from *Ferula kuhistanica*. Nat. Prod. 63, 362–365.

Costa, P., Yunes, R.A., Serrão, S.A., Malheiros, A., De Souza, M.M., 2003. Activity of *Rapanea ferruginea* on memory of normal animals and with Alzheimer induced by streptozotocin, V Simposio Iberoamericano de Plantas Medicinais. Itajai, Brazil.

Dong, M., Nagaoka, M., Miyazaki, S., Iriye, R., Hirota, M., 1999. 3-Geranyl-4-hydroxy-5-(3′-methyl-2′-butenyl)benzoic acid as an anti-inflammatory compound from *Myrsine seguinii*. Biosci. Biotechnol. Biochem. 63, 1650–1653.

Elamin, A.A., Ahlneck, C., Alderborn, G., Nystrom, C., 1994. Increased metastable solubility of milled griseofulvin, depending on the formation of a disordered surface structure. Int. J. Pharm. 111, 159–170.

Flores, N., Jiménez, I.A., Giménez, A., Ruiz, G., Gutiérrez, D., Bourdy, G., Bazzocchi, I.L., 2009. Antiparasitic activity of prenylated benzoic acid derivatives from Piper species. Phytochemistry 70, 621–627.

Gazoni, V.F., 2009. Análise fitoquímica e avaliação do efeito anticolinesterásico do extrato e compostos isolados da *Rapanea ferruginea*. Universidade do Vale do Itajaí, Itajaí.

Ghose, A.K., Viswanadhan, V.N., Wendoloski, J.J., 1999. A knowledge-based approach in designing combinatorial or medicinal chemistry libraries for drug discovery. 1. A qualitative and quantitative characterization of known drug databases. J. Comb. Chem. 1, 55–68.

Hadgraft, J., Plessis, J., Goosen, C., 2000. The selection of non-steroidal anti-inflammatory agents for dermal delivery. Int. J. Pharm. 207, 31–37.

Hattab, Y., Benharrats, N., 2015. Thermal stability and structural characteristics of PTHF–Mmt organophile nanocomposite. Arab. J. Chem. 8, 285–292.

Hess, S., Padoani, C., Scorteganha, L.C., Holzmann, I., Malheiros, A., Yunes, R.A., Delle-Monache, F., De Souza, M.M., 2010. Assessment of mechanisms involved in antinociception caused by myrsinoic acid B. Biol. Pharm. Bull. 33, 209–215.

Hirota, M., Miyazaki, S., Minakuchi, T., Takagi, T., Shibata, H., 2002. Myrsinoic acids B, C and F, anti-inflammatory compounds from *Myrsine seguinii*. Biosci. Biotechnol. Biochem. 66, 555–559.

ICH, 2005. Validation of Analytical Procedures: Text and Methodology – ICH Harmonized Tripartite Guideline.

Ito, S., Narise, A., Shimura, S., 2008. Identification of a methioninase inhibitor, Myrsinoic Acid B, from *Myrsine seguinii* Lév., and its inhibitory activities. Biosci. Biotechnol. Biochem. 72, 2411–2414.

Láng, P., Kiss, V., Ambrus, R., Farkas, G., Szabó-Révész, P., Aigner, Z., Várkonyi, E., 2013. Polymorph screening of an active material. J. Pharm. Biomed. Anal. 84, 177–183.

Makabe, H., Miyazaki, S., Kamo, T., Hirota, M., 2003. Myrsinoic acid E, an anti-inflammatory compound from *Myrsine seguini*. Biosci. Biotechnol. Biochem. 67, 2038–2041.

Malami, I., 2012. Prenylated benzoic acid derivatives from *Piper species* as source of anti-infective agents. Int. J. Pharm. Sci. Drug Res. 3, 1554–1559.

Martino, P., Censi, R., Barthélémy, C., Gobetto, R., Joiris, E., Masic, A., Odou, P., Martelli, S., 2007. Characterization and compaction behaviour of nimesulide crystal forms. Int. J. Pharm. 342, 137–144.

Maximiano, F.P., Costa, G.H.Y., Souza, J., Cunha-Filho, M.S.S., 2010. Caracterização físico-química do fármaco antichagásico benzonidazol. Quím. Nova 33, 1714–1719.

Mizushina, Y., Miyazaki, S., Ohta, K., Hirota, M., Sakaguchi, K., 2000. Novel anti-inflammatory compounds from *Myrsine seguinii*, terpeno-benzoic acids, are inhibitors of mammalian DNA polymerases. Biochim. Biophys. Acta 1475, 1–4.

OECD, 1989. Guideline for the Testing of Chemicals 117 – Partition Coefficient (n-octanol/water), High Performance Chromatography (HPLC) Method.

Pajouhesh, H., Lenz, G.R., 2005. Medicinal chemical properties of successful central nervous system drugs. NeuroRx 2, 541–553.

Seeram, N.P., Jacobs, H., Mcleant, S., Reynolds, W.F., 1996. Prenylated hydroxybenzoic acid derivatives from *Piper murrayanum*. Phytochemistry 43, 863–865.

Singh, P., Roberts, M.S., 1994. Concentrations of nonsteroidal anti-inflammatory drugs after topical application. J. Pharmacol. Exp. Ther. 268, 144–151.

Sonkusare, S.K., Kaul, C.L., Ramarao, P., 2005. Dementia of Alzheimer's disease and other neurodegenerative disorders: memantine, a new hope. Pharmacol. Res. 51, 1–17.

Sozio, P., Cerasa, L.S., Marinelli, L., Di Stefano, A., 2012. Transdermal donepezil on the treatment of Alzheimer's disease. Neuropsychiatr. Dis. Treat. 8, 361–368.

The United States Pharmacopeia and National Formulary, 2012. USP 35 – NF 30. USP 35 – NF 30. Rockville MD 20852. The United States Pharmacopeial Convention. US Pharmacopeia.

Vandenabeele, P., Wehling, B., Moens, L., Edwards, H., De Reu, M., Van Hooydonk, G., 2000. Analysis with micro-Raman spectroscopy of natural organic binding media and varnishes used in art. Anal. Chim. Acta 407, 261–274.